

Competing Orders and Spin-Density-Wave Instability in $\text{La}(\text{O}_{1-x}\text{F}_x)\text{FeAs}$

J. Dong, H. J. Zhang, G. Xu, Z. Li, G. Li, W. Z. Hu, D. Wu, G. F. Chen, X. Dai, J. L. Luo, Z. Fang,* and N. L. Wang†
*Beijing National Laboratory for Condensed Matter Physics, Institute of Physics,
 Chinese Academy of Sciences, Beijing 100080, People's Republic of China*

The interplay between different ordered phases, such as superconducting, charge or spin ordered phases, is of central interest in condensed matter physics. The very recent discovery of superconductivity with a remarkable $T_c=26$ K in Fe-based oxypnictide $\text{La}(\text{O}_{1-x}\text{F}_x)\text{FeAs}$ is a surprise to the scientific community[1]. The pure LaOFeAs itself is not superconducting but shows an anomaly near 150 K in both resistivity and dc magnetic susceptibility. Here we provide combined experimental and theoretical evidences showing that the anomaly is caused by the spin-density-wave (SDW) instability, and electron-doping by F suppresses the SDW instability and recovers the superconductivity. Therefore, the $\text{La}(\text{O}_{1-x}\text{F}_x)\text{FeAs}$ offers an exciting new system showing competing orders in layered compounds.

Both charge-density wave (CDW) and spin-density-wave (SDW) instabilities may develop in the presence of Fermi surface (FS) nesting[2], as shown in many transition metal compounds, such as 2H-NbSe_2 [3] and Cr [4]. The difference is that CDW couples to lattice and SDW couples to spin. The CDW or SDW instabilities may compete with other possible orderings, and complicated phase diagrams are often drawn due to their interplay. This is exactly what happens for LaOFeAs as shown in this paper. LaOFeAs crystalizes in layered square lattice with Fe layers sandwiched by two As layers (up and down), each Fe is coordinated by As tetrahedron. Its electronic properties are dominated by the (FeAs)-triple-layers, which contribute mostly to the electronic state around Fermi level (E_f). The electronic structure of LaOFeAs is quasi-two-dimensional and very similar to typical semi-metal, namely there are hole-like FS cylinders around the Γ -Z line of the Brillouin zone (BZ), and electron-like FS cylinders around the M-A line of the BZ (except a small 3D FS around the Z point of BZ) [5, 6, 7, 8, 9]. We will show here that surprisingly strong FS nesting exists by connecting the hole and electron FS by a commensurate vector $q=(\pi, \pi, 0)$. This leads to SDW instability, and it is the main cause of the anomaly observed at 150 K experimentally. The spontaneously symmetry-broken SDW state is characterized in terms of reduced carrier density due to (partial) FS nesting, enhanced conductivity due to the reduction of scattering channel, and loss of 4-fold rotational symmetry with negligible change of lattice.

Series of $\text{La}(\text{O}_{1-x}\text{F}_x)\text{FeAs}$ samples are fabricated, and Fig. 1 (a) shows the temperature dependence of the re-

sistivity. The pure LaOFeAs sample has rather high dc resistivity value and very weak temperature dependence at high temperature, but below roughly 150 K, the resistivity drops steeply, with an upturn at lower temperature (below 50 K). At 2% F-doping, the overall resistivity decreases and the 150 K anomaly shifts to the lower temperature and becomes less pronounced. At 3% F-doping, the anomaly could not be seen, and a superconducting transition occurs at $T_c=17$ K. With further increasing F content, and the superconducting transition temperature increases with the highest $T_c=28$ K seen at 6~8% F-doping. A T_c vs. F-content phase diagram is plotted in the inset of the figure 1 (a).

Apparently, superconductivity competes with the phase showing the anomaly in this system. To identify whether the anomaly at 150 K in LaOFeAs is due to a phase transition, we performed the specific heat measurement. Figure 1 (b) shows the specific heat data as a function of temperature. Very clear specific heat jump is seen at the temperature close to 155 K (see the expanded plot in the upper inset). A step-like, although broad, feature in the specific heat data suggests that the anomaly is caused by a second order phase transition. A good linear T^2 dependence indicates that the specific heat C is mainly contributed by electrons and phonons. The fit yields the electronic coefficient $\gamma=3.7$

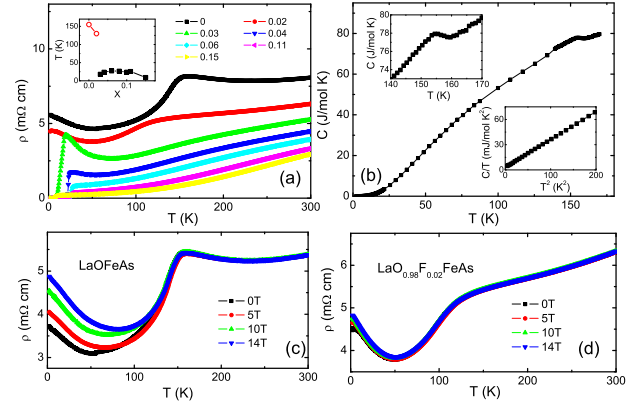


FIG. 1: (a) The electrical resistivity vs temperature for a series of $\text{LaO}_{1-x}\text{F}_x\text{FeAs}$. Inset: The phase diagram showing the anomaly (red circle) and superconducting transition (black square) temperatures as a function of F content. (b) specific heat vs temperature curve. Upper inset: the expanded region near the transition temperature; lower inset: a plot of C/T vs T^2 . (c) and (d) T -dependent resistivity under magnetic field for the pure and 2% F-doping samples, respectively.

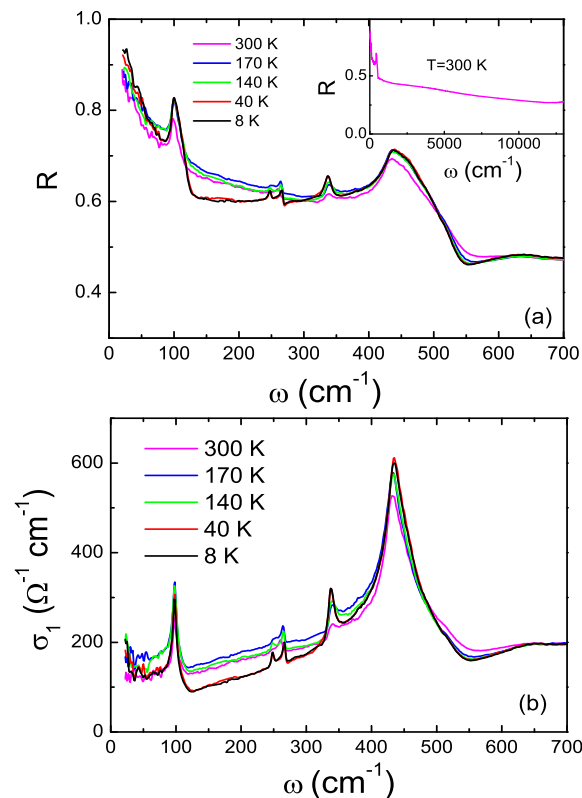


FIG. 2: (Color online) (a) The reflectance spectra in the far-infrared region at different temperatures for the pure LaOFeAs sample. The inset shows the reflectance over broad frequency range at room temperature. (b) The conductivity spectra at different temperatures.

mJ/mol·K² and the Debye temperature $\theta_D=282$ K. Note that the electronic coefficient γ is significantly smaller than the values obtained from the band structure calculations being about 5.5-6.5 mJ/mol·K². [6, 7] This result is unconventional, because usually the band structure calculation gives smaller value than the experimental data, their difference is ascribed to the renormalization effect. We recently measured a Ni-based oxypnictide La(O_{0.9}F_{0.1})NiAs, and indeed found that the experimental electronic coefficient is larger than the band structure calculation [10]. As we shall show below that a partial energy gap formation is revealed at the phase transition and explained as originated from the SDW instability, the smaller experimental value here could be naturally accounted for by the gap formation which removes parts of the density of states below the phase transition.

We also measured the resistivity under magnetic field. Figure 1 (c) and (d) shows the results for the pure and 2% F-doping samples, respectively. The anomaly transition temperature is rather insensitive to magnetic field up to 14 T, however sizable positive magnetoresistance are observed at low temperature for pure LaOFeAs. The positive magnetoresistance could be understood in terms

of the suppression of SDW order (and therefore enhanced spin scattering) by external magnetic field. After 2% F-doping, the low temperature magnetoresistance becomes much weaker, which suggests the same tendency that F-doping tries to suppress the anomaly around 150K. The overall picture is pretty much similar to the elemental Cr, a typical SDW system, where transition temperature is extremely insensitive to magnetic field and sizable magnetoresistance exists after SDW transition. [4]

Important information about the nature of the phase transition could be obtained from the optical measurement. Figure 2 (a) shows the temperature-dependence of the reflectance in the far-infrared region for the pure LaOFeAs sample. The reflectance at 300 K over broad frequency range is shown in the upper inset. Even though the measurement was performed on polycrystalline samples, two important experimental findings regarding to the phase transition could be unambiguously drawn from the measurement. First, below the phase transition temperature, the reflectance is strongly suppressed below the frequency of 400 cm⁻¹. This is dramatically different from the F-doped LaO_{0.9}F_{0.1- δ} FeAs superconducting sample where a monotonous increase of the reflectance was seen [11]. The suppression is a strong indication for the formation of an energy gap in the density of state. Note that the reflectance at very low frequency increases fast and exceeds the values at high temperature, e.g. above the phase transition. This indicates that the compound is still metallic even below the phase transition, being consistent with the dc resistivity measurement which reveals an enhanced conductivity. The data indicate clearly that only partial or some of the Fermi surfaces are gapped. We note that the gap is very small, roughly in the range of 150~350 cm⁻¹. Below 50 cm⁻¹, we find a sharp upturn for conductivity spectrum at 8 K (see fig. 2 (b)), suggesting development of very narrow Drude compound, which should be linked to the survived FS in the SDW state.

Second, a number of pronounced phonon structures are seen in the reflectance and conductivity spectra. Note that infrared spectroscopy probes phonon modes only near Γ point, the frequencies of the observed infrared active modes are basically in agreement with the calculations by Singh and Du. [6] Upon cooling the sample below the transition temperature, no new phonon mode is observed. [12] Considering the polycrystalline nature of the sample which has random orientations of the ab-plane and the c-axis, the absence of the any new phonon mode strongly suggests that there is no, or at least negligible, lattice distortion across the phase transition. Therefore, the phase transition could not be of CDW origin.

In the following we shall illustrate that the transition is caused by the SDW transition due to the Fermi surface nesting from first-principles calculations. Since only the magnetic translational symmetry has been broken, there is no modulation for the charge density, which can ex-

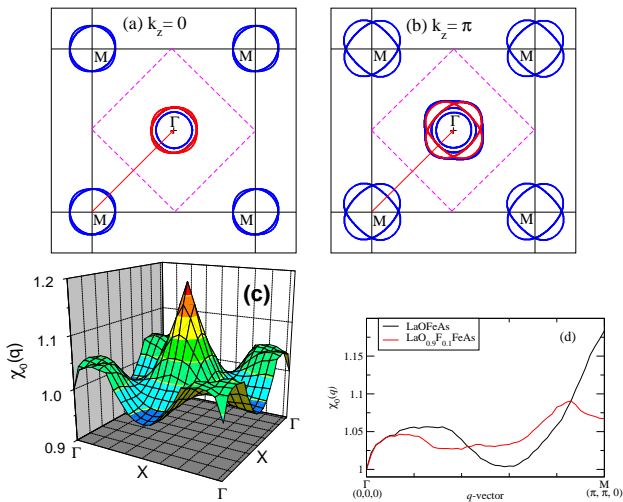


FIG. 3: (a) and (b) are the Fermi surfaces (FS) cutted at the $k_z=0$ and π planes respectively. The blue lines are original calculated FS, while red lines indicate the FS shifted by $q=(\pi, \pi, 0)$. Significant nesting is clear. (c) The calculated Lindhard response function $\chi_0(q)$. It is strongly peaked at M point. (d) The $\chi_0(q)$ along the Γ -M line. The peak at M point is much suppressed by F-doping.

plain the absence of new phonon modes appearing in the optical data after the transition. As we will show below, after the SDW transition, a stripe like spin ordering pattern appears which breaks the 4-fold rotational symmetry and induces a nematic order in the charge sector.

Using the experimental high temperature structure ($P4/nmm$ symmetry), our calculated electronic structures and Fermi surfaces are identical to those done by other people [5, 6, 7]. By cutting the BZ into fixed- k_z planes, circle like FS are resolved (as shown in Fig.3(a) and (b) for $k_z=0$ and $k_z=\pi$ planes respectively). Surprisingly, by shifting the circles around the M points to the Γ point, i.e. by a vector $q=(\pi, \pi, 0)$, the electron-like FS will largely overlap with the hole-like FS, suggesting significant nesting effect. For example, for the $k_z=0$ plane, the small electron circle almost exactly overlaps with the large hole circle after shifting by q . Similar thing happens for the $k_z=\pi$ plane. The nesting effect can be quantitatively estimated by calculating the Lindhard response function as shown in Fig 3(c) and (d). The calculated $\chi_0(q)$ is strongly peaked at M point for undoped compound, and it is much suppress by electron-doping, because the up-shift of Fermi level tends to reduce the size of hole-like FS and enlarge the electron FS. The existence of strong nesting effect would suggest that certain kinds of ordering, either CDW or SDW, may develop at low temperature. As mentioned above, the absence of any new phonon mode after the transition suggests that CDW modulation is unlikely, otherwise the structural distortion would lead to much more new phonon modes. Nevertheless, here we provide further theoretical

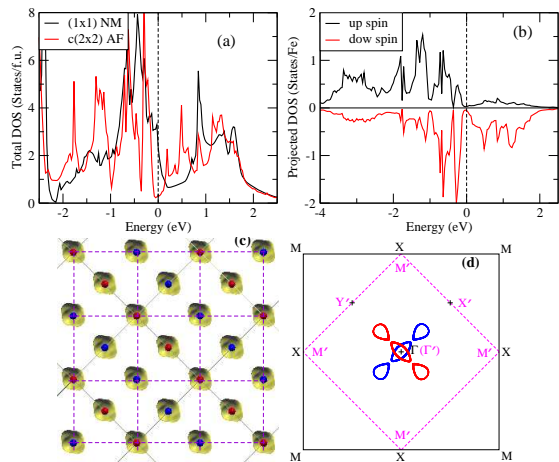


FIG. 4: (a) The total DOS of (1×1) NM and $(\sqrt{2}\times\sqrt{2})$ AF solutions. The reduction of $N(E_F)$ is about 7. (b) The projected DOS of Fe site for the AF solution. (c) The stripe-like ordering pattern of Fe plane and the charge distribution (occupied). The Fe atoms are indicated by red and blue spheres with up and down spin respectively. The original (1×1) unit cell is indicated by the dashed lines. (d) The calculated FS of AF state. The BZ special points of $(\sqrt{2}\times\sqrt{2})$ cell are indicated by symbols with prime. The red lines are rotated from blue lines, corresponding to the 90 degrees rotation of stripe orientation.

evidences.

The commensurate nesting vector suggests the doubling of the unit cell to be $(\sqrt{2}\times\sqrt{2})$ (i.e. the folding of the BZ along the dashed lines shown in Fig. 3 (a) and (b)), which is not treated by previous calculations [6, 7]. We have tried to optimized the structure of non-magnetic (NM) state without using any symmetry, the solution always recover to the original (1×1) structure. However, among several possible magnetic solutions, one antiferromagnetic (AF) ordered state (see the ordering pattern shown in Fig.4) can be stabilized with about 40 meV/Fe lowering in energy and about $1.5 \mu_B/\text{Fe}$ for the spin moment compared to (1×1) NM solution. Clearly the nesting instability likes to couple with spin rather charge. It is important to note that only part of the FS are nested, as the results, the system remains to be metallic and only partial gap opens at E_F . The density of state at E_F is reduced significantly compared with original (1×1) NM solution as shown in Fig. 4. All those factors are exactly what were observed in our experiments. Treating the F-doping by virtue crystal approximation, we found that both nesting effect and the stabilization energy of AF solution are suppressed, again explain the experimental observation.

The obtained AF ordered state is different with the (1×1) NM state in the sense that 4-fold rotational symmetry is broken due to the presence of magnetic ordering, and the stripe-like ordering pattern is revealed for the Fe plane (as shown in Fig. 4 (c)). However, if the stripe

orientation is rotated by 90 degrees for the neighboring Fe plane stacking along z , the lattice parameters may remain to be 4-fold invariant. Furthermore, if we concentrate on the charge (rather than magnetic density) distribution, the translational symmetry of total charge remains to be the same as original (1×1) structure (as shown in Fig. 4(c)). As we mentioned, this is the reason why no new phonon modes are observed. It deserves to remark that, in the ordered state, the charge at Fe site has a preferentially aligned distribution along stripe direction (see Fig. 4 (c)). The fact that charge density picks up of preferred direction after a spontaneous symmetry-breaking in spin sector could be considered as a formation of nematic order.[13] Here, the order is characterized by a 4-fold rotational symmetry broken.

Experiment:

The samples were prepared by the solid state reaction using Fe_2O_3 , Fe, La, As, and LaF_3 as starting materials. LaAs was obtained by reacting La chips and As pieces at 500°C for 15 hours and then 850°C for 2 hours. The raw materials were thoroughly mixed and pressed into pellets. The pellets were wrapped with Ta foil and sealed in an evacuate quartz tube under argon atmosphere. They were then annealed at 1150°C for 50 hours. The phase purity was checked by a powder X-ray diffraction method using $\text{Cu K}\alpha$ radiation at room temperature. The XRD patterns are well indexed on the basis of tetragonal ZrCuSiAs -type structure with the space group P4/nmm . The electrical resistivity was measured by a standard 4-probe method. The specific heat measurement was carried out using a thermal relaxation calorimeter. The heat capacity of addenda were carefully calibrated before measurement. All these measurements were performed down to 1.8K in a Physical Property Measurement System (PPMS) of Quantum Design company. Optical reflectance measurement were performed on Bruker 113v and 66v/s spectrometers in the frequency range from 20 cm^{-1} to $15,000\text{ cm}^{-1}$ at different temperatures. The samples were polished and shiny and metallic bright surface was obtained. An *in-situ* gold overcoating technique was used for the experiment. Optical conductivity was derived from Kramers-Kronig transformation of reflectance. The first-principles calculations were done using plane-wave pseudopotential method and generalized gradient approximation (GGA) for the exchange-correlation potential. For the 1×1 unit cell, the calculated results are identical to those performed by other people [6, 7].

We acknowledge the support from Y. P. Wang and

valuable discussions with Y. G. Yao and T. Xiang. This work is supported by the National Science Foundation of China, the Knowledge Innovation Project of the Chinese Academy of Sciences, and the 973 project of the Ministry of Science and Technology of China.

* Electronic address: zfang@aphy.iphy.ac.cn

† Electronic address: nlwang@aphy.iphy.ac.cn

- [1] Y. Kamihara, T. Watanabe, M. Hirano, and H. Hosono, "Iron-based layered superconductor $\text{La}[\text{O}_{1-x}\text{F}_x]\text{FeAs}$ ($x=0.05-0.12$) with $T_c=26\text{ K}$ ", *J. Am. Chem. Soc.* **130**, 3296 (2008).
- [2] G. Grüner, *Density waves in solids*, Addison-Wesley Pub. (1994).
- [3] Th. Straub, Th. Finteis, R. Claessen, P. Steiner, S. Hufner, P. Blaha, C. S. Oglesby, and E. Bucher, "Charge-density-wave mechanism in 2H-NbSe_2 : photoemission results", *Phys. Rev. Lett.* **82**, 4504 (1999).
- [4] see, for example, the review article, E. Fawcett, "Spin-density-wave antiferromagnetism in chromium", *Rev. Mod. Phys.* **60**, 209 (1988), and the references therein.
- [5] S. Lebégue, "Electronic structure and properties of the Fermi surface of the superconducting LaOFeP ", *Phys. Rev. B* **75**, 035110 (2007).
- [6] D. J. Singh and M. H. Du, " $\text{LaFeAsO}_{1-x}\text{F}_x$: A low carrier density superconductor near itinerant magnetism", arXiv:0803.0429v1.
- [7] Gang Xu, Wenmei Ming, Yugui Yao, Xi Dai, Shou-Cheng Zhang, and Zhong Fang, "Doping-dependent Phase Diagram of LaOMAs ($M=\text{V-Cu}$) and Electron-type Superconductivity near Ferromagnetic Instability", arXiv:0803.1282v2.
- [8] K. Haule, J. H. Shim, and G. Kotliar, "Correlated electronic structure of $\text{LaO}_{1-x}\text{F}_x\text{FeAs}$ ", arXiv:0803.1279v1.
- [9] I.I. Mazin, D.J. Singh, M.D. Johannes, and M.H. Du, "Unconventional sign-reversing superconductivity in $\text{LaFeAsO}_{1-x}\text{F}_x$ ", arXiv: 0803.2740v1.
- [10] Z. Li, G. F. Chen, J. Dong, G. Li, W. Z. Hu, J. Zhou, D. Wu, S. K. Su, P. Zheng, N. L. Wang, J. L. Luo, "Superconductivity in layered nickel-based $\text{LaO}_{1-x}\text{F}_x\text{NiAs}$ ", arXiv:0803.2572.
- [11] G. F. Chen, Z. Li, G. Li, J. Zhou, D. Wu, J. Dong, W. Z. Hu, P. Zheng, Z. J. Chen, J. L. Luo, N. L. Wang, "Superconducting properties of Fe-based layered superconductor $\text{LaO}_{0.9}\text{F}_{0.1-\delta}\text{FeAs}$ ", arXiv:0803.0128.
- [12] A phonon mode at 247 cm^{-1} is very weak at high temperature but eminently enhanced at low temperature. We have carefully checked two different samples, and concluded that the mode exists both below and above the phase transition.
- [13] E. Fradkin, S. Kivelson, V. Oganesyan, "Electron nematic phase in a transition metal oxide", *Science* **315**, 196 (2007).